Structures of $[(CO_2)_n(CH_3OH)_m]^-$ ($n = 1-4$, $m = 1, 2$) Cluster Anions

Azusa Muraoka, Yoshiya Inokuchi,† and Takashi Nagata*

Department of Basic Science, Graduate School of Arts and Sciences, The University of Tokyo, Komaba, Meguro-ku, Tokyo 153-8902, Japan

Received: January 12, 2008; Revised Manuscript Received: March 14, 2008

The infrared photodissociation spectra of $[(CO_2)_n(CH_3OH)_m]^-$ ($n = 1-4$, $m = 1, 2$) are measured in the 2700−3700 cm^{-1} range. The observed spectra consist of an intense broad band characteristic of hydrogen-bonded OH stretching vibrations at ≈3300 cm^{-1} and congested vibrational bands around 2900 cm^{-1}. No photofragment signal is observed for $[(CO_2)_{1,2}(CH_3OH)_1]^-$ in the spectral range studied. Ab initio calculations are performed at the MP2/6−311++G** level to obtain structural information such as optimized structures, stabilization energies, and vibrational frequencies of $[(CO_2)_n(CH_3OH)_m]^-$. Comparison between the experimental and the theoretical results reveals the structural properties of $[(CO_2)_n(CH_3OH)_m]^-$: (1) the incorporated CH_3OH interacts directly with either CO_2^- or $C_2O_4^-$ core by forming an O−H···O linkage; (2) the introduction of CH_3OH promotes charge localization in the clusters via the hydrogen-bond formation, resulting in the predominance of $CO_2^-\cdot(CH_3OH)_m(CO_2)_{n-1}$ isomeric forms over $C_2O_4^-\cdot(CH_3OH)_m(CO_2)_{n-2}$; (3) the hydroxyl group of CH_3OH provides an additional solvation cite for neutral CO_2 molecules.

Introduction

Since the first mass-spectrometric discovery of the hydrated anion of CO_2 by Klots,[1] stabilization of otherwise unstable gas-phase anions by "microhydration" has been the subject of a number of investigations.[2–9] Unveiling the physics behind the distinct stabilities of those gas-phase hydrated anions eventually leads to the microscopic understandings of various phenomena involving ionic species in solutions. The first step to be taken toward this end is to seek the structural information on the hydrated anions. In our previous study, the structures of $[(CO_2)_n(H_2O)_m]^-$ ($n = 1-4$, $m = 1, 2$) were investigated by infrared photodissociation (IPD) spectroscopy combined with ab initio calculations.[10] The IPD measurement in the spectral region of hydrogen-bonded OH stretching vibrations (3000−3800 cm^{-1}) has revealed that (1) the incorporated H_2O preferably forms a double ionic hydrogen-bonding (DIHB) configuration with $C_2O_4^-$ (configuration **1** or **2** in Scheme 1) as a structural subunit in the $[(CO_2)_n(H_2O)_1]^-$ species and that (2) additional introduction of H_2O preferentially stabilizes CO_2^- by the formation of two OH···O linkages (configuration **3** or **4**) in $[(CO_2)_n(H_2O)_2]^-$. For the descriptive convenience, the $[(CO_2)_n(H_2O)_m]^-$ species containing CO_2^- are hereafter referred to as "type I", and those containing $C_2O_4^-$ are referred to as "type II" after ref 11. In the type I structure, the excess electron is localized on a CO_2 monomer, whereas the electron is delocalized over two CO_2 constituents to form $C_2O_4^-$ in the type II structure.

The extent of charge delocalization within the cluster anions is primarily governed by the competition between stabilization attained by solvent-induced charge localization and the intrinsic tendency toward charge delocalization through resonance interactions. As H_2O interacts strongly with charge-concentrated moieties through hydrogen-bond formation, the introduction of H_2O into $(CO_2)_n^-$ would promote charge localization substantially within the clusters. Contrary to this expectation, our previous study showed that type II structures still dominated in $[(CO_2)_n(H_2O)_1]^-$ ($n = 2-4$) and that the introduction of another H_2O was needed for the CO_2^- formation.[10,11] As readily seen from the structural "motifs" displayed in Scheme 1, the exceptional stability of type II isomers ($C_2O_4^-$ core) of the $[(CO_2)_n(H_2O)_1]^-$ species is ascribable to the occurrence of configuration **1**; this originates from the unique ability of H_2O to form DIHB configurations. Thus, the intrinsic propensity for charge localization by hydrogen-bond formation is somewhat blurred in $[(CO_2)_n(H_2O)_m]^-$.

SCHEME 1

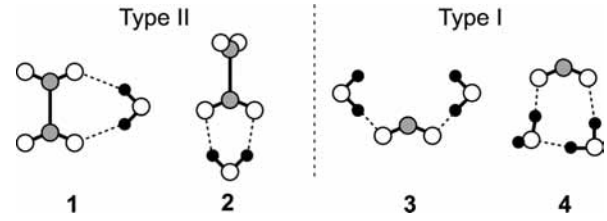

In the present study, we apply IPD spectroscopy to $[(CO_2)_n(CH_3OH)_m]^-$ ($n = 1-4$, $m = 1, 2$). The IPD spectra are measured in the 2700−3700 cm^{-1} range, providing information on the hydrogen-bonds formed in $[(CO_2)_n(CH_3OH)_m]^-$. As CH_3OH can be thought as being the simplest protic molecule with one hydroxyl group, it is expected that the hydrogen-bonded structures of $[(CO_2)_n(CH_3OH)_m]^-$ simply reflect the role of the protic solvent as a charge-localization promoter as well as an anion stabilizer. Ab initio calculations for $[(CO_2)_n(CH_3OH)_m]^-$ are also performed at the MP2/6−311++G** level. The calculations provide optimized geometries for $[(CO_2)_n(CH_3OH)_m]^-$ along with their vibrational frequencies, which can be compared directly with the experimental IPD spectra. On the basis of the IPD spectral features in conjunction with the ab initio results, the structural properties of $[(CO_2)_n(CH_3OH)_m]^-$ are discussed in terms of the solvent-induced charge localization and stabilization.

* Corresponding author. E-mail: nagata@cluster.c.u-tokyo.ac.jp.
† Present address: Department of Chemistry, Graduate School of Science, Hiroshima University, Kagamiyama, Higashi-Hiroshima, Hiroshima 739-8526, Japan.

10.1021/jp800289g CCC: $40.75
Published on Web 05/08/2008

Experimental and Theoretical Methods

The IPD spectra of $[(CO_2)_n(CH_3OH)_m]^-$ are measured by an ion-guide spectrometer equipped with a tandem quadrupole mass filter.[12] The target $[(CO_2)_n(CH_3OH)_m]^-$ is prepared as follows. A gas mixture of carbon dioxide and methanol (a total stagnation pressure of $1-2 \times 10^5$ Pa) is introduced into the vacuum chamber through a pulsed nozzle (General Valve Series 9) with a repetition rate of 10 Hz. The pulsed free jet is crossed with a continuous electron beam at the exit of the nozzle, resulting in the production of secondary slow electrons. These electrons are attached to neutral $(CO_2)_N(CH_3OH)_M$ clusters in the beam to form the $[(CO_2)_n(CH_3OH)_m]^-$ anions:

$$(CO_2)_N(CH_3OH)_M + e^- \rightarrow [(CO_2)_N(CH_3OH)_M]^{*-} \rightarrow [(CO_2)_N(CH_3OH)_m]^- + (N-n)CO_2 + (M-m)CH_3OH \quad (1)$$

In process 1, the nascent $[(CO_2)_N(CH_3OH)_M]^{*-}$ species are stabilized by evaporative cooling;[13] the $[(CO_2)_n(CH_3OH)_m]^-$ products are likely to possess a sizable, but small enough to keep from dissociation, amount of internal energy. Hence, the sample preparation method employed here provides a condition where low-lying $[(CO_2)_n(CH_3OH)_m]^-$ isomers coexist in the free jet. After passing through a skimmer, the ions are accelerated into the first quadrupole mass filter by a 50 eV pulsed voltage. Mass-selected ions of interest are then introduced into a quadrupole ion guide through a 90° ion bender. The ion beam is merged with an output of a pulsed infrared photodissociation laser in the ion guide. Resultant fragment ions are mass-analyzed by the second quadrupole mass filter and detected by a secondary electron multiplier tube. The IPD spectra of the parent ions are obtained by plotting the yields of fragment ions against wavenumber of the dissociation laser. The dissociation channel monitored for obtaining the IPD spectra of $[(CO_2)_n(CH_3OH)_m]^-$ is the loss of one CO_2 molecule except for $[(CO_2)_1(CH_3OH)_2]^-$; one CH_3OH is ejected upon the infrared irradiation on $[(CO_2)_1(CH_3OH)_2]^-$.

The tunable infrared source used in this study is an optical parametric oscillator system (Continuum Mirage 3000) pumped with an injection-seeded Nd:YAG laser (Continuum Powerlite 9010). The output energy is about 1−2 mJ pulse^{-1} with a line width of ≈1 cm^{-1}. The infrared laser is loosely focused into the ion guide by using a CaF_2 lens ($f = 1000$ mm).

Ab initio molecular orbital (MO) calculations are carried out with the Gaussian 98 program package[14] in order to estimate the structural and spectroscopic properties of $[(CO_2)_n(CH_3OH)_m]^-$, such as optimized geometries, vibrational frequencies, and total energies. Geometry optimization and vibrational frequency analysis are performed at the MP2/6−31+G* and MP2/6−311++G** levels of theory. Both levels of theory have provided primarily identical and consistent results for optimized geometries and vibrational frequencies. In this article, we employ the optimized structures and vibrational frequencies obtained by the MP2/6−311++G** calculations for spectral assignments. To compare the calculated vibrational frequencies with observed ones, a scaling factor of 0.9404 is employed for all of the frequencies calculated. This factor is determined so as to reproduce the OH stretching vibrational frequencies of a free CH_3OH molecule. For saving CPU time without sacrificing seriously our pursuit of accuracy, the total energies of $[(CO_2)_n(CH_3OH)_m]^-$ are evaluated by the single-point energy calculations at the CCSD(T)/6−31+G* level with the optimized structures given by the MP2/6−31+G* calculations (CCSD(T)/6−31+G*//MP2/6−31+G*).

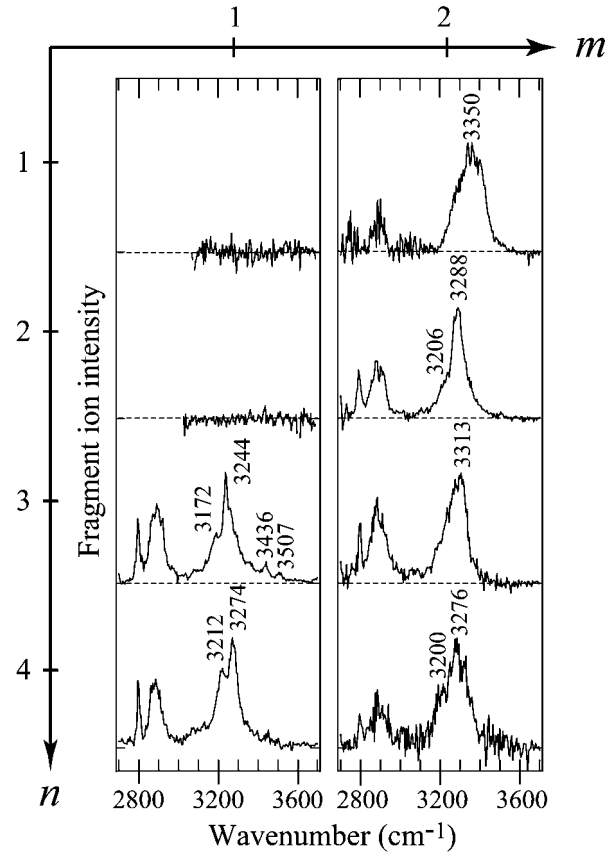

Figure 1. Overview of the infrared photodissociation spectra of $[(CO_2)_n(CH_3OH)_m]^-$ measured in the 2700−3700 cm^{-1} range. The numbers n, m in the figure denote the composition of $[(CO_2)_n(CH_3OH)_m]^-$.

Results and Discussion

A. Infrared Photodissociation Spectra of $[(CO_2)_n(CH_3OH)_m]^-$. Figure 1 presents an overview of the IPD spectra of $[(CO_2)_n(CH_3OH)_m]^-$ with $n = 1-4$, and $m = 1, 2$ measured in the 2700−3700 cm^{-1} range. Except for the $(n, m) = (1, 1)$ and (2, 1) spectra, where the fragment signals were indiscernible, the IPD spectra possess similar features in the observed spectral range, that is, a sharp band at 2800 cm^{-1}, a somewhat broad band around 2900 cm^{-1}, and an intense broad band spreading over the range of 3100−3400 cm^{-1}. The similarity in these spectral features, especially in the spectral region associated with the OH-stretching vibration (3000−3700 cm^{-1}), indicates that the $[(CO_2)_n(CH_3OH)_m]^-$ species investigated here contain a similar type of hydrogen-bonded structure.

From the overview displayed in Figure 1, we infer that the intense broad band at ≈3300 cm^{-1} in each spectrum is assignable to the hydrogen-bonded OH stretching vibration of CH_3OH; the spectral position is shifted significantly toward lower frequencies from that of the OH stretching vibration of gas-phase CH_3OH (3681 cm^{-1}).[15] This assignment is further confirmed by checking the absence of the ≈3300 cm^{-1} band in the IPD spectra of $[(CO_2)_n(CH_3OD)_m]^-$ measured under the identical conditions. The spectral features in the 2800−3000 cm^{-1} range are found to be rather insensitive to the size and the composition of $[(CO_2)_n(CH_3OH)_m]^-$. We are able to assign the 2800 and 2900 cm^{-1} bands to the vibrations of the methyl group of CH_3OH, on the basis of their spectral positions and the assignments reported in literature.[15] As the 2800−3000 cm^{-1} features give only little information on the hydrogen-bonded structures of $[(CO_2)_n(CH_3OH)_m]^-$, we will focus our interest on the spectral features in the 3000−3700 cm^{-1} range hereafter.

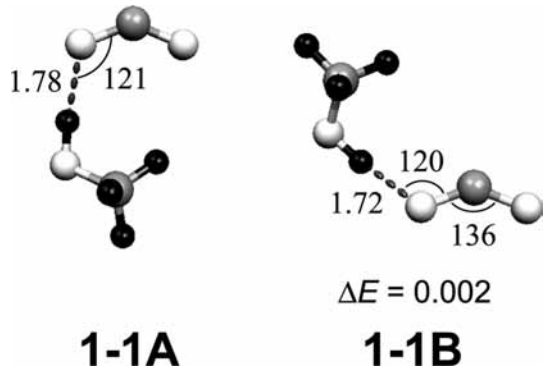

Figure 2. Optimized geometries for $[(CO_2)_1(CH_3OH)_1]^-$ obtained at the MP2/6−311++G** level. Bond lengths and angles are given in units of Angstroms and degrees unless otherwise noted.

B. Spectral Assignments. ***1. $[(CO_2)_n(CH_3OH)_1]^-$.*** Although we could not detect any IPD signal for $[(CO_2)_1(CH_3OH)_1]^-$, hydrogen-bonded structures for $[(CO_2)_1(CH_3OH)_1]^-$ are still deemed worthy of considering as the prototypical ones. As shown in Figure 2, ab initio calculations predict the existence of two stable isomeric forms for $[(CO_2)_1(CH_3OH)_1]^-$ at the MP2/6−311++G** level. The structures shown in Figure 2 are essentially identical to those obtained previously by the MP2/6−31+G* calculations.[16] The isomeric forms denoted as **1−1A** and **1−1B** are almost equal in energy. The total energies of the isomers differ from each other only by 0.002 eV, which is obviously a tiny quantity not only beyond the accuracy of the CCSD(T)/6−31+G*//MP2/6−31+G* calculations but also inconsiderable compared with the amount of internal energy deposited in $[(CO_2)_1(CH_3OH)_1]^-$. Hereafter, we use the notation "***n*−*m*X**" in referring to each isomeric form, where the first digit of "***n*-*m*X**" represents the number n of CO_2 molecules involved in the cluster anion, the second digit, the number m of CH_3OH molecules, and the last character "**X**" is for identifying the individual structure. The frequencies of the hydrogen-bonded OH stretching vibrations are calculated to be 3272 and 3218 cm^{-1} for **1−1A** and **1−1B**, respectively, both of which lie in the spectral range investigated. The absence of IPD signals for $[(CO_2)_1(CH_3OH)_1]^-$ is ascribable either to the large bond dissociation energy for the CO_2^- + CH_3OH channel or to the instability of the possible photoproduct CO_2^-. The amount of energy required for the hydrogen-bond dissociation is estimated to be 0.69 eV for **1−1A**, which is well above the infrared-photon energies employed in the present study (2700−3700 cm^{-1}, 0.33−0.46 eV). As discussed above, however, the $[(CO_2)_n(CH_3OH)_m]^-$ species are produced internally "hot" under the present beam conditions. We cannot rule out the possibility that the internally hot species dissociate upon the infrared-photon absorption. If this is the case, the product CO_2^- might elude the detection due possibly to its short lifetime (<100 μs).[17]

The ab initio energies and the vibrational frequencies obtained for $[(CO_2)_1(CH_3OH)_1]^-$ are listed in Table 1. In Table 1, all of the present ab initio results referred to in the following discussion are summarized for readers' convenience.

As already seen in Figure 1, also $[(CO_2)_2(CH_3OH)_1]^-$ does not provide IPD signals. The present ab initio calculations predict the existence of eight stable isomeric forms for $[(CO_2)_2(CH_3OH)_1]^-$ at the MP2/6−311++G** level. In Figure 3, three of them are shown as the lowest-energy representatives of the isomeric forms having different hydrogen-bonded structures. Forms **2−1B** and **2−1C** belong to the type I structure (CO_2^- core), and **2−1A** belongs to the type II structure ($C_2O_4^-$ core), with the energy ordering of **2−1A** ≈ **2−1B** < **2−1C**

TABLE 1: Ab initio Energies and Harmonic Vibrational Frequencies of $[(CO_2)_n(CH_3OH)_m]^-$

(n, m)	isomer	total energy[a] (Hartree)	ΔE[b] (eV)	dissociation energy[c] (eV)	υ_{calc}[d] (cm^{-1})
(1, 1)	**1−1A**	−303.517 66	0.000	0.691	3272
	1−1B	−303.517 58	0.002	0.688	3218
(2, 1)	**2−1A**	−491.663 75	0.000	0.397	3512
	2−1B	−491.663 47	0.008	0.387	3209
	2−1C	−491.661 22	0.069	0.326	3180
(3, 1)	**3−1A**	−679.808 14	0.000	0.386	3253
	3−1B	−679.807 16	0.027	0.329	3182
	3−1C	−679.805 75	0.065	0.361	3020
	3−1D	−679.806 01	0.058	0.290	3526
	3−1E	−679.804 86	0.089	0.267	3463
(1, 2)	**1−2A**	−418.928 15	0.000	0.653	3075, 3375
	1−2B	−418.927 86	0.008	0.645	3336, 3361
	1−2C	−418.927 81	0.009	0.644	3304, 3345
(2, 2)	**2−2A**	−607.074 06	0.000	0.399	3318, 3348
	2−2B	−607.073 05	0.028	0.370	3265, 3354
	2−2C	−607.071 62	0.066	0.332	3222, 3365
	2−2D	−607.071 48	0.070	0.327	3265, 3366

[a] Total energies evaluated by single-point CCSD(T)/6−31+G*//MP2/6−31+G* calculations. [b] Relative energies with reference to the most stable structure. [c] Dissociation energies for the minimum-energy demanding channels leading to a loss of CH_3OH for (1, 1) and (1, 2), while to a loss of CO_2 for (2, 1), (3, 1), and (2, 2). [d] Vibrational frequencies for H-bonded O−H stretches calculated at the MP2/6−311++G** level. For theoretical IR intensities, refer to the plots in Figures 4−6.

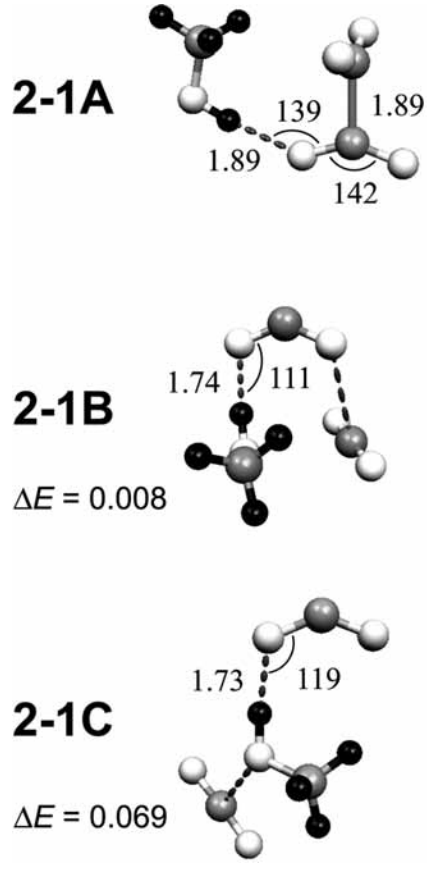

Figure 3. Optimized geometries for $[(CO_2)_2(CH_3OH)_1]^-$ obtained at the MP2/6−311++G** level.

(ΔE = 0.069 eV). The energy difference, ΔE, is defined as the amount of total energy with respect to the most stable structure. The calculations predict the bond dissociation energy for the least energy-demanding channel, $[(CO_2)_2(CH_3OH)_1]^-$ →

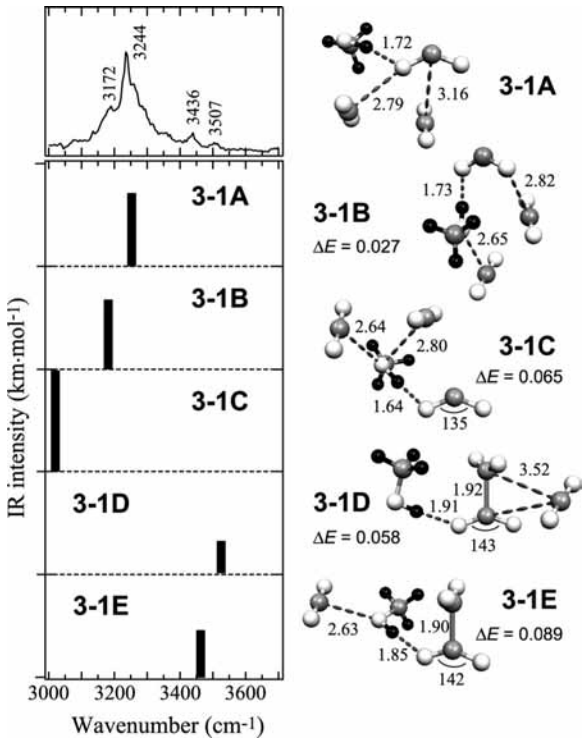

Figure 4. Infrared photodissociation spectrum of $[(CO_2)_3(CH_3OH)_1]^-$ (top panel) compared with the calculated vibrational spectra for $[(CO_2)_3(CH_3OH)_1]^-$ isomers. One unit in the ordinate of the calculated spectra corresponds to the IR intensity of 1500 km·mol^{-1}. Also shown on the right side are the corresponding optimized structures of the $[(CO_2)_3(CH_3OH)_1]^-$ isomers.

$CO_2^-\cdot CH_3OH + CO_2$, to be 0.40, 0.39, and 0.33 eV for **2**−**1A**, **2**−**1B**, and **2**−**1C**, respectively. The calculated frequencies of the hydrogen-bonded OH stretching vibrations are 3512 cm^{-1} for **2**−**1A**, 3209 cm^{-1} for **2**−**1B**, and 3180 cm^{-1} for **2**−**1C**. Apparently, the absence of IPD signals cannot be elucidated in terms of the bond dissociation energies and the spectral positions. At the present stage, this issue remains to be explained.

The $[(CO_2)_3(CH_3OH)_1]^-$ anion is the smallest member of the $[(CO_2)_m(CH_3OH)_1]^-$ series which undergoes vibrational predissociation into fragment anions via the infrared excitation. The IPD signals were detected as the loss of one CO_2 from $[(CO_2)_3(CH_3OH)_1]^-$. In Figure 4, the IPD spectrum of $[(CO_2)_3(CH_3OH)_1]^-$ in the 3000−3700 cm^{-1} range is compared with the vibrational spectra calculated for possible isomeric forms. The main band of the IPD spectrum is composed of at least two components, one of which is located at 3244 cm^{-1} and the other at ≈3170 cm^{-1} as a shoulder. Besides these bands, tiny peaks appear at 3436 and 3507 cm^{-1}. Considering that each band component corresponds to the specific OH oscillation of a certain isomeric form, we can infer that at least four types of isomeric forms contribute to the observed IPD spectrum. The MP2/6−311++G** calculations provide 23 possible geometries for $[(CO_2)_3(CH_3OH)_1]^-$; 18 isomers belong to type I and the remaining 5 are of type II structure. In all of these calculated isomeric forms, a hydrogen bond is formed between CH_3OH and the O atom of either the CO_2^- or the $C_2O_4^-$ core. In Figure 4, the five representative isomeric forms taking on different types of solvation structures are also shown. In **3**−**1A**, CH_3OH interacts with the CO_2^- core through an OH···O hydrogen bond and two CO_2 act as solvent interacting directly with the ionic core. As is the case with $(CO_2)_n^-$, the solvent−core interaction arises from an effective overlap between the $2\pi_u$ (LUMO) orbital of CO_2 and either the $4b_2$ (HOMO) or the $6a_1$ (SOMO) orbital of CO_2^-.[18] The $4b_2$ orbital is localized on the O atoms of CO_2^-. The $6b_2$ orbital, primarily localized on the C atom of CO_2^-, extends its electron lobe mainly along the bisector of the angle ∠OCO. This solvent−core interaction scheme gives a qualitative understanding of the solvation structures of **3**−**1A**. In **3**−**1B**, one neutral CO_2 interacts with the O atom of CH_3OH instead of CO_2^-, while in **3**−**1C**, two CO_2 do. In the type II isomers, **3**−**1D** and **3**−**1E**, the CO_2 solvent attaches either to the $C_2O_4^-$ core or to the O site of CH_3OH. As represented by **3**−**1A** through **3**−**1E**, the solvation structures are eventually categorized according to (1) the type of ionic core and (2) the number of CO_2 molecules attached to CH_3OH. Referring to each category of solvation structures, we introduce a new notation, T^i, where T (= I or II) represents the type of ionic core (CO_2^- or $C_2O_4^-$) and the suffix i is the number of CO_2 interacting with CH_3OH. For example, the structural category of **3**−**1A** is referred to as I^0, and that of **3**−**1E** is referred to as II^1. The ab initio calculations also reveal that frequencies of the OH stretching vibration are almost the same for the isomeric forms belonging to the same category of solvation structure (Table 1).

Getting back to the comparison between the observed IPD spectrum and the calculated ones in Figure 4, the 3244 cm^{-1} band is ascribable to **3**−**1A**, on the basis of its spectral position. The position of the weak shoulder (3172 cm^{-1}) coincides fairly well with the calculated frequency of the OH vibration of **3**−**1B** (3182 cm^{-1}). The 3436 and 3507 cm^{-1} bands are ascribable to the type II isomers, **3**−**1E** and **3**−**1D**, of which calculated frequencies are 3463 and 3526 cm^{-1}. As no discernible vibrational band appears around the spectral position expected for **3**−**1C** (3020 cm^{-1}), we infer that **3**−**1C** has negligible population in $[(CO_2)_3(CH_3OH)_1]^-$. Note that **3**−**1A**, **3**−**1B**, **3**−**1D**, and **3**−**1E** are the minimum energy representatives of the I^0, I^1, II^0 and II^1 families of $[(CO_2)_3(CH_3OH)_1]^-$, respectively. For example, the ab initio calculations provide five isomeric forms (ΔE = 0.01−0.05 eV), other than **3**−**1A**, belonging to I^0; their calculated OH vibrational frequencies are located in the range 3250−3280 cm^{-1}. Hence, we infer that these I^0 family members as well as **3**−**1A** contribute to the observed broad band at 3244 cm^{-1} under the present beam condition. The situation should be the same with **3**−**1B**, **3**−**1D**, and **3**−**1E**: not only the minimum-energy structure of each family but also the low-lying family members serve as spectral carriers.

From the above spectral assignments for $[(CO_2)_3(CH_3OH)_1]^-$, one can derive some sort of propensity rules regarding the spectral positions: (1) OH oscillator interacting with CO_2^- vibrates at a lower frequency than that interacting with $C_2O_4^-$; (2) Addition of one CO_2 on the OH oscillator reduces the frequency by 60−70 cm^{-1}, irrespective of the type of interacting ionic core. Item (1) is possibly due to the fact that the OH oscillator interacts through an OH···O linkage more strongly with the CO_2^- core because the negative charge is concentrated on the O atoms more in CO_2^- (Mulliken charge ≈ −0.6) than in $C_2O_4^-$ (≈ −0.4). There seems to be no straightforward explanation for item (2). These propensity rules are also applicable to other $[(CO_2)_n(CH_3OH)_m]^-$ systems, as will be discussed below.

It is also interesting to note that type II isomers, **3**−**1D** and **3**−**1E**, are detected in the present measurement, although the previous photoelectron spectroscopic study gave no evidence for the existence of type II isomers in $[(CO_2)_3(CH_3OH)_1]^-$.[11] The IRD measurement proves to be more sensitive to the

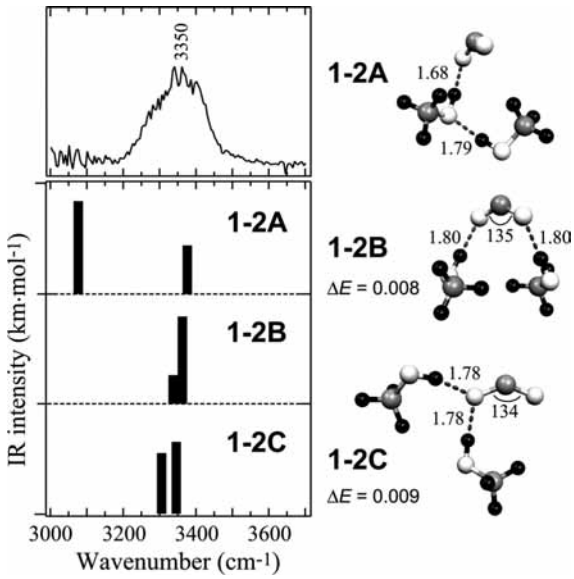

Figure 5. Infrared photodissociation spectrum of $[(CO_2)_1(CH_3OH)_2]^-$ (top panel) compared with the calculated vibrational spectra for $[(CO_2)_1(CH_3OH)_2]^-$ isomers. One unit in the ordinate of the calculated spectra corresponds to the IR intensity of 1500 km·mol^{-1}. Also shown on the right side are the corresponding optimized structures of the $[(CO_2)_1(CH_3OH)_2]^-$ isomers.

presence of electronic isomers in $[(CO_2)_n(CH_3OH)_m]^-$, as has already been demonstrated by Shin et al. in the $(CO_2)_n^-$ study.[19]

As for the $[(CO_2)_4(CH_3OH)_1]^-$ species, we could not complete ab initio calculations due first to a formidable computational time at the MP2/6−311++G** level and, second, to the increasing number of possible isomeric forms for $[(CO_2)_4(CH_3OH)_1]^-$. This prevents us from a direct comparison between observed and calculated spectra in the $n = 4$ case. The observed $[(CO_2)_4(CH_3OH)_1]^-$ spectrum consists of two components at 3212 and 3274 cm^{-1} (Figure 1). By comparing the spectral features between $[(CO_2)_3(CH_3OH)_1]^-$ and $[(CO_2)_4(CH_3OH)_1]^-$, and considering the above propensity rules, we assign the 3212 and 3274 cm^{-1} components respectively to the hydrogen-bonded OH vibrations of the I^1 and I^0 family members of $[(CO_2)_4(CH_3OH)_1]^-$.

2. [(CO₂)ₙ(CH₃OH)₂]⁻. The $[(CO_2)_1(CH_3OH)_2]^-$ spectrum is characterized by a remarkably broadened band around 3350 cm^{-1} (Figure 5), which cannot be resolved into components. Among 12 isomeric forms predicted by the MP2/6−311++G** calculations, 3 forms are selectively quoted in Figure 5; they are the lowest-energy representatives of the $[(CO_2)_1(CH_3OH)_2]^-$ isomers with different solvation structures. All of these isomeric forms gain their stabilization energies by forming two hydrogen bonds. In isomer **1−2A**, one hydrogen bond is formed between the CO_2^- core and CH_3OH, while the other is formed between two CH_3OH molecules. In **1−2B**, the O atoms on both sides of the CO_2^- core take part in the hydrogen-bond formation with two CH_3OH molecules, while both CH_3OH make O−H···O linkages with the O atom on one side of the ionic core in **1−2C**. The CCSD(T)/6−31+G* calculations predict **1−2A** through **1−2C** to be almost isoenergetic.

As readily seen in Figure 5, the calculated spectral patterns for **1−2B** and **1−2C** reasonably match the IPD spectral features. The position of the higher-frequency band of **1−2A** (3375 cm^{-1}) almost coincides with the observed value of ≈3350 cm^{-1}, whereas the other vibrational transition expected to occur at 3075 cm^{-1} is not observed in the present measurement. Hence, the observed IPD band is assigned eventually to the hydrogen-bonded OH oscillations of **1−2B**, **1−2C**, and their isomer families. A noteworthy feature of the vibration motions in **1−2B** and **1−2C** is that two OH oscillators are coupled together forming either an in-phase or an out-of-phase hydrogen-bonded OH stretching vibrational mode. In the in-phase mode, two H atoms move back and forth along their O−H···O linkages in a coherent manner, which gives rise to the 3361 cm^{-1} transition for **1−2B**, and 3345 cm^{-1} for **1−2C**. In the out-of-phase mode, one O−H bond stretches while the other compresses; this mode corresponds to the 3336 cm^{-1} band of **1−2B**, and the 3304 cm^{-1} band of **1−2C**. The large oscillator strength for the 3361 cm^{-1} transition arises possibly from a large magnitude of $(\partial\mu/\partial Q_1)$ for the in-phase O−H stretching motions in **1−2B**.

It is also worth comparing the above assignments with those made for the hydrogen bonds in $X^-(CH_3OH)_m$ (X = F, Cl, I),[20−22] especially in terms of methanol−methanol hydrogen-bond formation. According to the arguments for the hydrogen-bonded structures of $X^-(CH_3OH)_m$, the 3075 cm^{-1} transition predicted for **1−2A** can be categorized as the stretching vibration of a "cooperatively enhanced" ionic hydrogen bond between the anionic core and CH_3OH. The second solvent CH_3OH enhances the first ionic H bond between CO_2^- and CH_3OH, leading to the additional frequency shift of ≈300 cm^{-1} relative to the "nonenhanced" ionic O−H stretching vibration (≈3350 cm^{-1}). Hence, the absence of the 3075 cm^{-1} transition in the $[(CO_2)_1(CH_3OH)_2]^-$ spectrum directly indicates the absence of the intersolvent hydrogen bond in $[(CO_2)_1(CH_3OH)_2]^-$. This spectral interpretation seems to be quite reasonable as compared to the facts that the onset for methanol−methanol H bonding was observed at $m = 4$ in the $F^-(CH_3OH)_m$ and $Cl^-(CH_3OH)_m$ systems[20,21] and that the cooperatively enhanced ionic hydrogen bond is formed preferentially in cold, argon-solvated $I^-(CH_3OH)_2$.[22]

The infrared-photodissociation of $[(CO_2)_1(CH_3OH)_2]^-$ occurs with a loss of one CH_3OH in the present study. The threshold energy for $[(CO_2)_1(CH_3OH)_2]^- \rightarrow [(CO_2)_1(CH_3OH)_1]^- + CH_3OH$ is calculated to be 0.65 eV for **1−2B** and 0.64 eV for **1−2C**; these values substantially exceed the energy delivered by the 2700−3700 cm^{-1} infrared photons. Again, the $[(CO_2)_1(CH_3OH)_2]^-$ species prepared in the electron-impact ionized jet retain internal energies enough to dissociate upon the single photon absorption. This might also cause the broadness of the IPD band in the $[(CO_2)_1(CH_3OH)_2]^-$ spectrum. Not only the hot bands of specific isomers such as **1−2B** and **1−2C** but also the vibrational bands of all of the isomeric forms with small ΔE can contribute to the IPD spectral features.

The $[(CO_2)_2(CH_3OH)_2]^-$ spectrum exhibits an IPD band at 3288 cm^{-1}, which is accompanied by a shoulder at ≈3200 cm^{-1} (Figure 6). The spectral shape of the 3288 cm^{-1} band is much sharper than that of $[(CO_2)_1(CH_3OH)_2]^-$ and rather resembles the 3244 cm^{-1} band shape of $[(CO_2)_3(CH_3OH)_1]^-$ (see Figure 4). From this observation, we infer that each CH_3OH molecule interacts directly with the CO_2^- core via a hydrogen bond and consequently that the propensity rules proposed in the previous section are applicable to the $[(CO_2)_2(CH_3OH)_2]^-$ case. According to the propensity rules, it can be inferred that type II isomers, whose vibrational bands would otherwise appear around 3500 cm^{-1}, make a negligible contribution to the $[(CO_2)_2(CH_3OH)_2]^-$ spectrum. In the geometry optimization at the MP2/6−311++G** level, 34 possible isomeric forms are obtained for $[(CO_2)_2(CH_3OH)_2]^-$; 27 isomers out of them have type I structure and the remaining 7 have type II structure. Among these type I isomers, 17 forms meet the above condition that both CH_3OH are hydrogen-bonded directly to CO_2^-. In Figure 6, shown are

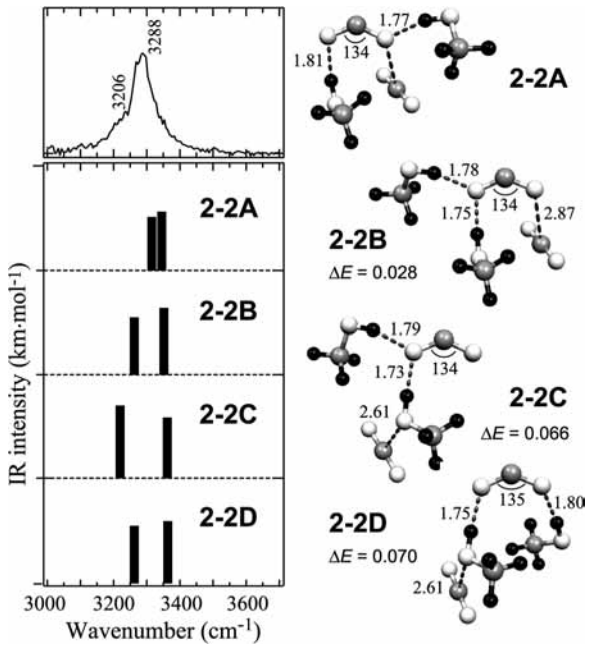

Figure 6. Infrared photodissociation spectrum of $[(CO_2)_2(CH_3OH)_2]^-$ (top panel) compared with the calculated vibrational spectra for $[(CO_2)_2(CH_3OH)_2]^-$ isomers. One unit in the ordinate of the calculated spectra corresponds to the IR intensity of 1500 km·mol^{-1}. Also shown on the right side are the corresponding optimized structures of the $[(CO_2)_2(CH_3OH)_2]^-$ isomers.

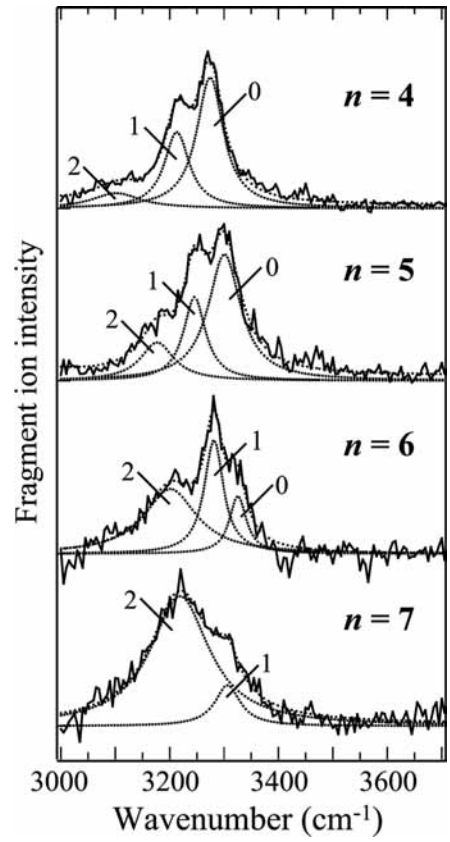

Figure 7. Infrared photodissociation spectra of $[(CO_2)_n(CH_3OH)_1]^-$ ($n = 4-7$). The solid lines represent the experimental data. The dotted curves are the Lorentzian components in the spectral deconvolution processing. The digits "0", "1" and "2" indicate the components attributed to the isomeric forms of categories I^0, I^1, and I^2, respectively.

the representatives for the 17 isomeric forms. As is the case with $[(CO_2)_1(CH_3OH)_2]^-$, two CH_3OH molecules are separately hydrogen bonded to the O atoms on each side of CO_2^- (isomer **2−2A**, **2−2D**), or together to the O atom on one side of CO_2^- (isomer **2−2B**, **2−2C**). Isomer **2−2A** and **2−2D** differ in the position of CO_2 solvation: neutral CO_2 interacts with the CO_2^- core in **2−2A** (category I^0), while it interacts with the hydroxyl group of CH_3OH in **2−2D** (category I^1). The situation is the same with **2−2B** and **2−2C**. The energy ordering is **2−2A** < **2−2B** < **2−2D** < **2−2C**. From the comparison between observed and calculated spectra in Figure 6, we conclude that the IPD bands are ascribable to the $[(CO_2)_2(CH_3OH)_2]^-$ isomeric forms as typified by **2−2A** through **2−2D**. The infrared-photodissociation of $[(CO_2)_2(CH_3OH)_2]^-$ leads to the production of $[(CO_2)_1(CH_3OH)_2]^-$ fragments, which is consistent with the ab initio results: the threshold energy for $[(CO_2)_2(CH_3OH)_2]^- \rightarrow [(CO_2)_1(CH_3OH)_2]^- + CO_2$ is calculated to be in the range of 0.33−0.40 eV for **2−2A** through **2−2D**.

Moving on to $[(CO_2)_n(CH_3OH)_2]^-$ with $n = 3$ and 4, we see from Figure 1 that the main features of the IPD spectra displayed in $n = 1$ and 2 still remain in the large-n species although the band profiles are somewhat broadened. This implies that the hydrogen-bonded structures emerging in the $n = 1$ and 2 species retain their motifs in the larger $[(CO_2)_n(CH_3OH)_2]^-$ with $n = 3$ and 4. The broadness of the IPD bands in the $[(CO_2)_3,_4(CH_3OH)_2]^-$ spectra arises possibly from the increasing number of coexisting isomers which undergo vibrational transitions around 3300 cm^{-1}. We have not performed ab initio calculations for these larger cluster anions; their geometry optimization and frequency analysis are definitely beyond our computational ability.

C. Structural Evolution in $[(CO_2)_n(CH_3OH)_m]^-$. To summarize the spectral assignments discussed above, solvation structures formed in $[(CO_2)_n(CH_3OH)_m]^-$ ($n = 1-4$, $m = 1, 2$) are characterized as follows: (i) each CH_3OH is hydrogen-bonded directly to the O atom of either the CO_2^- or the $C_2O_4^-$ core; (ii) the CH_3OH solvation tends to stabilize CO_2^- more efficiently than $C_2O_4^-$, leading to the predominance of type I isomers over type II at (n, m) = (3, 1), (4, 1), (2, 2), (3, 2), and (4, 2); and (iii) the hydroxyl group of CH_3OH provides an additional solvation cite for CO_2 attachment. These characteristics mark a sharp contrast with those of $[(CO_2)_n(H_2O)_m]^-$, especially in terms of core stabilization. In $[(CO_2)_n(H_2O)_m]^-$ with (n, m) = (2, 1), (3, 1), and (2, 2), $C_2O_4^-$ is preferentially stabilized by forming a DIHB configuration, where H_2O bridges two CO_2 moieties of the $C_2O_4^-$ core so as to reinforce the C−C bond formation (configuration **1**).[10] Thus, decreasing populations of type II isomers in $[(CO_2)_n(CH_3OH)_m]^-$ can be attributed to the intrinsic inability of CH_3OH to form a DIHB configuration.

Another aspect of the solvation structures that should be dealt with here is the structural evolution in $[(CO_2)_n(CH_3OH)_m]^-$ with an increase of the number of neutral CO_2. Figure 7 shows the IPD spectra for $[(CO_2)_n(CH_3OH)_1]^-$ with $n = 4-7$ in the 3000−3700 cm^{-1} range. As an aid for further discussion, spectral deconvolution processing has been performed, and the results are displayed in Figure 7: the profile of each IPD band is approximately reproduced by a superposition of two or three Lorentzian functions, each of which corresponds to the OH vibration inherent to a specific hydrogen-bonded structure. As has been discussed in section B.2, the components labeled with "0" and "1" in the top panel of Figure 7 are assignable to the hydrogen-bonded OH vibrations in $[(CO_2)_4(CH_3OH)_1]^-$ isomers having I^0 and I^1 structures, respectively. The deconvolution processing has also revealed the existence of a tiny but significant component at ≈3100 cm^{-1} in the $n = 4$ spectrum.

This component can be assigned to a hydrogen-bonded OH vibration of CH_3OH with two CO_2 interacting with the O atom of the hydroxyl group, on the basis of the propensity rules for spectral shifts by CO_2 solvation. Hence, we infer that there exist $n = 4$ isomeric forms which belong to a structural category labeled as I^2 according to the T^i nomenclature. As for $n = 5$ and 6, the IPD bands consist of three Lorentzian components ascribable to the solvation structures of categories I^0, I^1, and I^2, respectively, as is the case with $n = 4$. The spectral position of each component shifts toward higher frequencies with increasing number n: for example, the band center of the I^0 component is located at 3274 cm^{-1} for $n = 4$, 3302 cm^{-1} for $n = 5$, and 3326 cm^{-1} for $n = 6$. This spectral shift arises possibly from the decreasing charge concentration on the CO_2^- core with increasing the number of solvating molecules; the more the charge is delocalized by solvation, the more the hydrogen bond weakens and, as a result, the OH stretching frequency is increased.

The relative intensities of three Lorentzian components at each cluster size also change with n, indicating that the relative abundance of the I^0, I^1, and I^2 structures depends on the cluster size. The isomers in category I^0 have the largest population at $n = 4$, while the population is significantly reduced at $n = 6$. The isomers in category I^2 show an opposite behavior, as clearly seen in Figure 7. From these observations, it can be inferred that the solvation structures of $[(CO_2)_n(CH_3OH)_1]^-$ evolve with n in such a way that I^0 structures are preferred more in smaller sizes with $n \leq 5$, whereas I^2 structures become dominant in the size range $n \geq 6$. In the $n = 7$ spectrum, the intensity of the I^0 component becomes negligible. The negligible population, or rather its absence, of I^0 structures suggests that the first solvation shell around the $OCO^-\cdots HOCH_3$ unit is closed at $n = 7$. In the shell-closed structure of $[(CO_2)_7(CH_3OH)_1]^-$, one CO_2 plays a role of the ionic core making an O···HO hydrogen bond with CH_3OH, another CO_2 interacts with the O atom of the OH group, and the remaining five CO_2 neutrals occupy the solvation cites around the CO_2^-core.

Conclusion

In summary, we report on the infrared photodissociation (IPD) spectra of binary cluster anions composed of carbon dioxide and methanol, $[(CO_2)_n(CH_3OH)_m]^-$ ($n = 1-4$, $m = 1, 2$). All of the observed IPD spectra, except for $(n, m) = (1, 1)$ and (1, 2), are characterized by intense broad bands around 3300 cm^{-1}, which are assigned to the hydrogen-bonded OH stretching vibrations of CH_3OH. The (1, 1) and (1, 2) species provide no photofragment signal in the spectral range investigated. Ab initio MO calculations have been carried out in order to obtain the optimized structures, vibrational frequencies, and total energies of $[(CO_2)_n(CH_3OH)_m]^-$. The spectral analyses with the aid of the ab initio results reveal that $[(CO_2)_n(CH_3OH)_m]^-$ isomeric forms responsible for the observed IPD spectra take on distinct structural motifs, where all of the CH_3OH molecules are directly bonded to either the CO_2^- or the $C_2O_4^-$ core via O−H···O hydrogen linkage(s). It is also revealed that type I structures (CO_2^- core) are preferentially stabilized by CH_3OH solvation in all of the $[(CO_2)_n(CH_3OH)_m]^-$ species which undergo infrared-photodissociation in the present study. The IPD bands ascribable to type II isomers ($C_2O_4^-$ core) are observed only at $(n, m) = (3, 1)$. This shows a striking contrast with the $[(CO_2)_n(H_2O)_m]^-$ case, where type II isomers appear as dominant species at $(n, m) = (2, 1)$, (3, 1), and (4, 1). The abundance of type I isomers in $[(CO_2)_n(CH_3OH)_m]^-$ arises mainly from the fact that localization of the excess charge in the CO_2^- moiety, rather than delocalization over $C_2O_4^-$, is favorable for strong hydrogen-bond formation. The findings in the present study first exhibit the intrinsic ability of a hydrogen bond to influence the charge localization/delocalization in molecular aggregates, and second, demonstrate afresh the unique ability of water as a solvent to form DIHB configurations.

Acknowledgment. The authors are grateful to Professor K. Takatsuka for the loan of high-performance computers, which enabled us to carry out a large amount of calculations. Professor H. Ushiyama and Dr. Y. Arasaki are also acknowledged for their technical help in the computation. A part of the ab initio calculations was performed by using the computer systems (NEC SX-7) at Research Center for Computational Science, Okazaki Research Facilities, National Institutes of Natural Sciences (NINS). This work was supported by Grants-in-Aid for Scientific Research (Grants 18550007 and 19029011) from Japan Society for the Promotion of Science (JSPS), and from the Ministry of Education, Culture, Sports, Science and Technology (MEXT).

Supporting Information Available: Structure parameters for the $[(CO_2)_n(CH_3OH)_m]^-$ isomeric forms shown in Figures 2, 3, 4, 5, 6 (MP2/6−311++G**). This material is available free of charge via the Internet at http://pubs.acs.org. The structure parameters for all the isomeric forms obtained in the present study are also available on request; the total numbers of optimized structures are 2, 10, 23, 12, and 34 for $(n, m) =$ (1, 1), (2, 1), (3, 1), (1, 2) and (2, 2), respectively.

References and Notes

(1) Klots, C. E. *J. Chem. Phys.* **1979**, *71*, 4172.
(2) Desfrancois, C.; Abdoul-Carime, H.; Schermann, J. P. *J. Chem. Phys.* **1996**, *104*, 7792.
(3) Hendricks, J. H.; Lyapustina, S. A.; de Clercq, H. L.; Bowen, K. H. *J. Chem. Phys.* **1998**, *108*, 8.
(4) Schiedt, J.; Weinkauf, R.; Neumark, D. M.; Schlag, E. W. *Chem. Phys.* **1998**, *239*, 511.
(5) Han, S. Y.; Song, J. K.; Kim, J. H.; Oh, H. B.; Kim, S. K. *J. Chem. Phys.* **1999**, *111*, 4041.
(6) Periquet, V.; Moreau, A.; Carles, S.; Schermann, J. P.; Desfrancois, C. *J. Electron Spectrosc. Relat. Phenom.* **2000**, *106*, 141.
(7) Lyapustina, S. A.; Xu, S.; Nilles, J. M.; Bowen, K. H. *J. Chem. Phys.* **2000**, *112*, 6643.
(8) Wang, X.-B.; Nicholes, J. B.; Wang, L.-S. *J. Chem. Phys.* **2000**, *113*, 10837.
(9) Morgado, C. A.; Pichugin, K. Y.; Adamowicz, L. *Phys. Chem. Chem. Phys.* **2004**, *6*, 2758.
(10) Muraoka, A.; Inokuchi, Y.; Nishi, N.; Nagata, T. *J. Chem. Phys.* **2005**, *122*, 094303.
(11) Tsukuda, T.; Saeki, M.; Kimura, R.; Nagata, T. *J. Chem. Phys.* **1999**, *110*, 7846.
(12) Inokuchi, Y.; Nishi, N. *J. Chem. Phys.* **2001**, *114*, 7059.
(13) Klots, C. E. *J. Chem. Phys.* **1985**, *83*, 5854.
(14) *Gaussian 98, Revision A. 11.4*, Frish, M. J.; Trucks, G. W.; Schlegel, H. B.; Scuseria, G. E. Robb, M. A.; Cheeseman, J. R.; Zakrzewski, V. G.; Montgomery, J. A., Jr.; Stratmann, R. E.; Burant, J. C.; Dapprich, S.; Millam, J. M., Daniels, A. D.; Kudin, K. N.; Strain, M. C.; Farkas, O.; Tomasi, J.; Barone, V.; Cossi, M.; Cammi, R.; Mennucci, B.; Pomelli, C.; Adamo, C.; Clifford, S.; Ochterski, J.; Petersson, G. A.; Ayala, P. Y., Cui, Q.; Morokuma, K.; Rega, N.; Salvador, P.; Dannenberg, J. J.; Malick, D. K. Rabuck, A. D.; Raghavachari, K.; Foresman, J. B.; Cioslowski, J.; Ortiz, J. V.; Baboul, A. G.; Stefanov, B. B.; Liu, G.; Liashenko, A.; Piskorz, P.; Komaromi, I.; Gomperts, R.; Martin, R. L.; Fox,D. J., Keith, T., Al-Laham, M. A., Peng, C. Y.; Nanayakkara, A.; Challacombe, M.; Gill, P. M. W.; Johnson, B.; Chen, W.; Wong, M. W.; Andres, J. L.; Gonzalez, C.; Head-Gordon, M.; Replogle, E. S. and Pople, J. A. Gaussian, Inc.: Pittsburgh, PA, 2002.
(15) Serrallah, A.; Meyer, R.; Günthard, Hs. H. *J. Mol. Spectrosc.* **1974**, *52*, 94.
(16) Saeki, M.; Tsukuda, T.; Iwata, S.; Nagata, T. *J. Chem. Phys.* **1999**, *111*, 6333.
(17) Cooper, C. D.; Compton, R. N. *J. Chem. Phys.* **1977**, *67*, 1779.

(18) Saeki, M.; Tsukuda, T.; Nagata, T. *Chem. Phys. Lett.* **2001**, *340*, 376.

(19) Shin, J.-W.; Hammer, N. I.; Johnson, M. A.; Schneider, H.; Glola, A.; Weber, J. M. *J. Phys. Chem. A* **2005**, *109*, 3146.

(20) Corbett, C. A.; Martínez, T. J.; Lisy, J. M. *J. Chem. Phys.* **1979**, *110*, 9516.

(21) Cabarcos, O. M.; Weinheimer, C. J.; Martínez, T. J.; Lisy, J. M. *J. Phys. Chem. A* **2002**, *106*, 10015.

(22) Robertson, W. H.; Karapetian, K.; Ayotte, P.; Jordan, K. D.; Johnson, M. A. *J. Chem. Phys.* **2002**, *116*, 4853.

JP800289G